CPX SIMULATOR: DEVELOPMENT OF A HYBRID SIMULATION MODEL OF THE CPX METHOD

Reto Pieren[1], Axel Heusser[1], Dominik Wöllstein[1], Sophia Feriani[1], Hazael Montanaro[1], Urs Pachale[1]

[1] *Empa, Swiss Federal Laboratories for Materials Science and Technology, Dübendorf, Switzerland*

Abstract

The close-proximity (CPX) method according to ISO 11819-2 is increasingly applied to monitor and characterize road surfaces. To better understand the physical mechanisms underlying CPX measurements and to enable predictions of CPX spectra, a hybrid simulation model called CPX simulator is developed. This contribution presents experimental and numerical investigations conducted during model development. First, an experimental approach to quantify the influence of the tire tread pattern on CPX spectra is introduced. The results reveal that the tread pattern of the used standard reference test tire (SRTT) plays a decisive role, particularly for smooth pavements at low driving speeds. The horn effect of a loaded tire is simulated using 3D FDTD. The simulations highlight the impact of the circumferential tire grooves and the acoustic impedance of the pavement on CPX spectra. The influence of the CPX trailer enclosure was examined through narrowband measurements using an artificial sound source. The observed distinct trailer influence at low frequencies can be well reproduced with a modal sound field description. Finally, predictions with the CPX simulator are compared to CPX measurements performed in Switzerland on various pavement types at different driving speeds. The comparisons confirm that the hybrid model accurately captures the combined influences of speed, pavement surface texture, and pavement impedance on spectral CPX levels.

Keywords: *tire/road noise, pavement, close-proximity method, simulation*

1. Introduction

The close-proximity (CPX) method according to the standard ISO 11819-2 [1] is increasingly applied to monitor and characterize road surfaces [2], [3], [4]. To better understand the physical mechanisms underlying CPX measurements and to enable predictions of CPX spectra, a hybrid simulation model called *CPX simulator* is developed.
This paper gives an overview of this model with an emphasis on some of the development work. The model concept is introduced in Section 2. Section 3 presents model developments and Section 4 some first verifications results.

2. Concept of the CPX simulator

The functional concept of the CPX simulator model is illustrated in Fig. 1. The model takes pavement properties as input as well as known influencing factors on CPX measurements such as driving speed, temperature and rubber hardness of the tire. As an output it provides sound pressure level spectra at the CPX microphone positions.

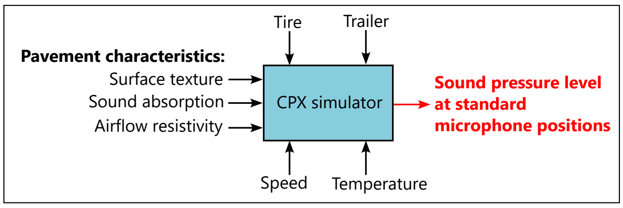

Figure 1: Functional concept of the CPX simulator calculation model.

The CPX simulator belongs to the class of hybrid models (see literature review by Li [5]) because it consists of a combination of mechanistic, i.e. physics-based components and on empirical, i.e. experimentally determined components. The modular structure representing different sound generation mechanisms, radiation and propagation is shown in Fig. 2.

3. Developments

In this section, we present experimental and numerical investigations conducted during model development,

Corresponding author: *reto.pieren@empa.ch.*

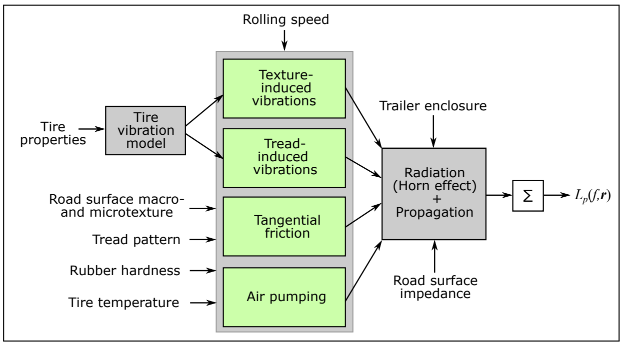

Figure 2: Structural framework of the hybrid calculation model CPX simulator to predict spectral sound pressure levels L_p.

which are specific to the CPX method. Our contributions are related to the tread pattern of the measurement tire, the horn effect at the CPX positions and the trailer influence.

3.1. Experimental separation of tread pattern and texture noise

Today, the ISO method uses two different measurement tires specified in ISO/TS 11810-3 [6]. The measurement tire intended to represent passenger car tires is the standard reference test tire (SRTT) defined in ASTM-F2492 [7]. We suspected that the tread pattern of the SRTT is a relevant factor for sound generation in CPX measurements. To study this experimentally, we developed and implemented a strategy to separate tread pattern noise and texture noise during CPX measurements. The principle is inspired by the works by Li et al. [8], [9] and illustrated in Fig. 3. We assume that due to repeated tire rotation, the tread pattern excites the tire structure periodically leading to tread pattern noise. In contrast, the random surface structure of common asphalts excites the tire stochastically resuling in texture noise. Those statistically different excitation features are used for signal decomposition of sound pressure signals.

We installed electromechanical switches on the wheel axles to generate trigger signals which are used to synchronize the recorded sound pressure signals to the tire revolution. A narrowband spectrum of such a rotation-synchronised microphone signal is shown in Fig. 4. In this example, distinct spectral peaks show up at the harmonics of the rotation frequency. These peaks are related to tread pattern noise. From the narrowband spectrum, the energy contribution of each peak is estimated (red shaded areas in Fig. 4) and used to dissect the measured sound pressure levels into tread pattern and texture noise within each 1/3 octave band.

We found that the tread pattern of the SRTT can have a substantial impact on measured sound pressure levels, particularly on smooth surfaces and at 50 km/h. Therefore, tread pattern noise is explicitly considered in the CPX simulator.

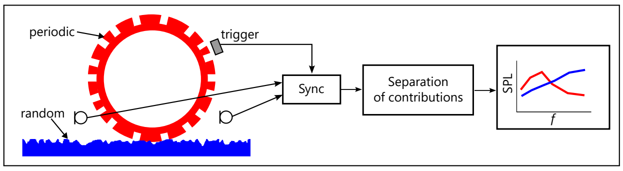

Figure 3: Concept of the experimental separation of tread pattern and texture noise contributions of CPX microphone signals.

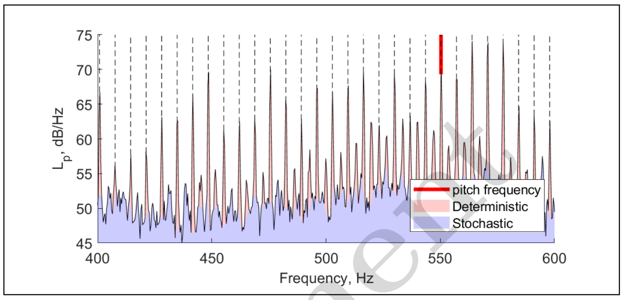

Figure 4: Narrowband spectrum of rotation-synchronised microphone signal at the CPX position 1 of a measurement with an SRTT tire at 50 km/h on a smooth pavement. Indication of rotational harmonics (dashed lines) and attribution to deterministic and stochastic pressure contributions (shaded areas).

3.2. Horn effect

The horn effect strongly depends on frequency, radiation direction and ground impedance [10]. We model the horn effect of a loaded tire numerically in 3D with the Finite-Difference-Time-Domain (FDTD) method using the in-house developed GPU-accelerated solver *sonora*. A spatial resolution of 2 mm is used to capture the tire curvature and tread geometry, and to cover the full frequency range of the CPX method. An example field snapshot is shown in Fig. 5.

From such simulations, the horn effect is evaluated assuming two incoherent point sources at the leading and trailing contact patch edge, respectively. The horn amplification at the standard CPX microphone positions is shown in Fig. 6 for a fully reflecting flat road surface. The horn effect for the CPX configuration is small below 400 Hz, but it becomes relevant and variable within the frequency range of the CPX method, i.e. between the 315 Hz and the 5 kHz 1/3 octave band, with a substantial amplification of 12 dB at 1 kHz. Simulation results are shown for three tire geometries: the SRTT, the SRTT with only its circumferential grooves and a slick tire, all with the same tire dimensions. Comparing these simulation results, the influence of the tread pattern on the radiation can be well observed, as recently investigated experimentally by Li et al. [11]. The four circumferential grooves of the SRTT lead to an amplification in the order of 3 dB in the important 1 kHz region.

By changing the boundary conditions of the ground plane underneath the tire geometry, the effect of the pavement surface impedance on the radiation is con-

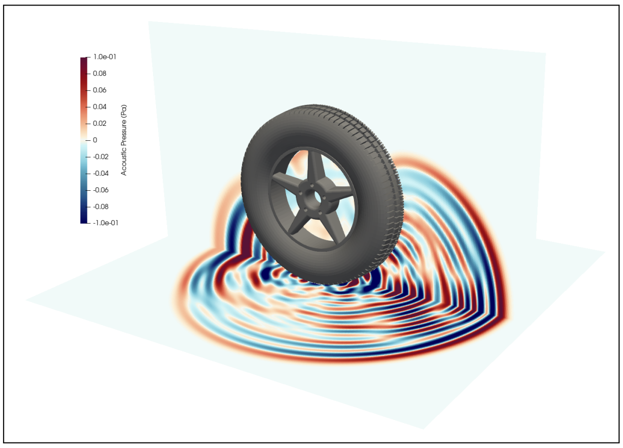

Figure 5: Sound pressure field around a loaded SRTT simulated with 3D FDTD. Sound pressure on two visualization planes at 2.3 ms after impulse excitation from a point source.

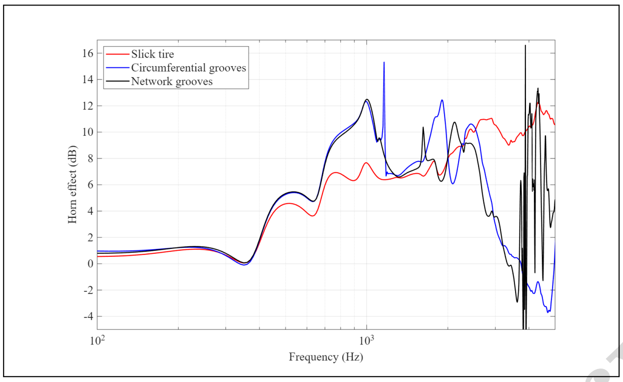

Figure 6: Simulated horn effect at the standard CPX microphone positions for three tires with different tread patterns on fully reflective ground. Tires: Full SRTT tread geometry (network grooves), SRTT with only its circumferential grooves, and slick tire.

sidered in the numerical simulation. As an example, Fig. 7 compares the horn effect on five absorbing surfaces ($\alpha_0 = \{0.05; 0.1; 0.2; 0.4; 0.8\}$) to a fully reflective surface. The results show that the finite impedance of the ground substantially reduces the horn effect above 400 Hz compared to a fully reflective road surface. For example, at the 1 kHz peak, the horn effect decreases by remarkable 5 dB for a surface with an absorption coefficient α_0 of only 0.2.

3.3. Trailer influence

Sound radiated from the tire propagates inside the trailer enclosure where it is reflected at the interior surfaces. The influence of the trailer enclosure on the sound pressure level at the CPX microphone positions was examined in the lab experimentally using an artificial tire-like source as specified in ISO 11819-2 (see Fig. 8). The interior surfaces of the enclosure of the studied CPX trailer (CoMeT CPX-XXL, M+P) are covered with a 51 mm layer of porous acoustic

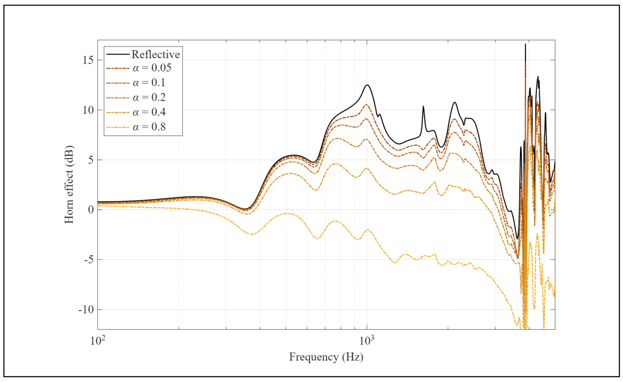

Figure 7: Simulated horn effect for the full SRTT at the mandatory CPX microphone positions (1 and 2) for six different road surfaces: five absorbing surfaces and a fully reflective surface.

foam. Narrowband measurements of the trailer influence are shown in Fig. 9. The trailer presence in some frequency regions leads to an amplification, in some frequency regions to an attenuation. The latter indicates destructive interference and reveals that an energy-based analysis is insufficient; instead, a phase-sensitive approach is required to describe the sound field in the trailer enclosure for the low frequency range of the CPX method.
Following a theoretical wave-based approach from room acoustics of small rooms [12], we modeled the sound field in the trailer enclosure using a modal description:

$$p(\omega, \mathbf{r}) = \rho_0 c^2 \omega Q \sum_n \frac{p_n(\mathbf{r}) p_n(\mathbf{r}_S)}{[2\delta_n \omega_n + i(\omega^2 - \omega_n^2)] K_n} \tag{1}$$

with the angular frequency ω, location $\mathbf{r}$, air density ρ_0 and speed of sound c, source volume velocity Q and source location $\mathbf{r_S}$, the imaginary unit i, modal indices n, the modal eigenfunctions p_n and their corresponding eigenfrequencies ω_n, a normalization factor K_n, and the modal damping constants δ_n. We measured the absorption coefficient α_0 of samples of the porous foam in an impedance tube according to ISO 10534-2 [13]. The absorption data was used to estimate the modal damping per mode.
Considering only the vertical modes, we could well reproduce the measured trailer influence up to 600 Hz (Fig. 9). The observed amplification of 4 dB at 370 Hz is due to a resonance. This resonance is only weakly damped because the absorption of the porous layer is relatively low at this frequency ($\alpha_0 = 0.45$). The attenuation observed at 300 Hz and at 500 Hz is due to a weak modal support, or in other words, due to destructive interference of reflected waves.

4. Verification

For the development and verification of the CPX simulator, we performed measurements on different pavement types in Switzerland. CPX measurements were

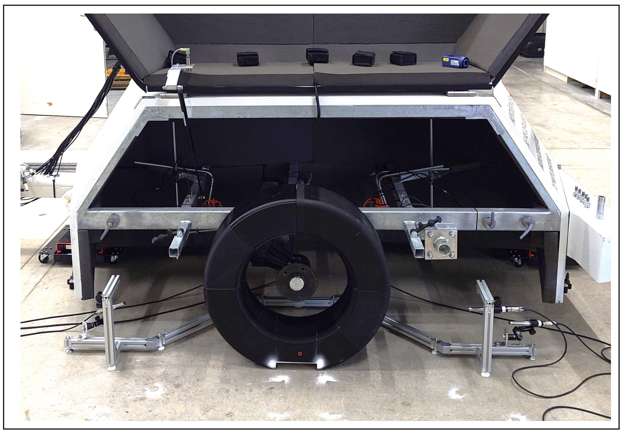

Figure 8: Measurement of the trailer enclosure influence with an artificial tire-like source and a microphone jig on a concrete floor. The trailer door was closed during the measurements.

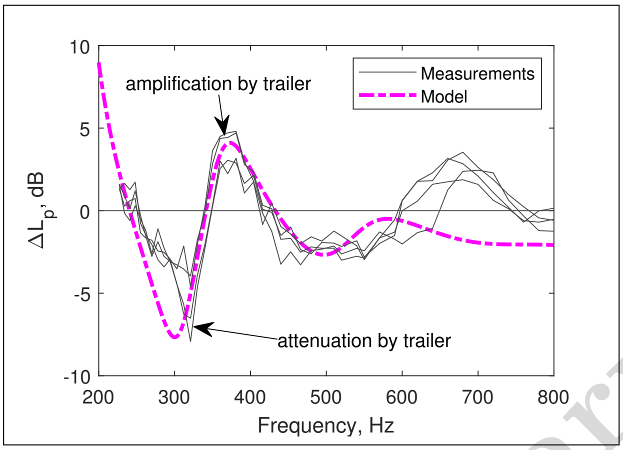

Figure 9: Trailer influence spectra from 200 to 800 Hz: Comparison of narrowband measurements (positions 1 and 2 of both sides of the trailer) and model calculation with modal description.

made with a set of two SRTTs at different driving speeds (CoMeT CPX-XXL from M+P; PAK Mk. II from Müller-BBM). As inputs to the model, we measured in-situ surface texture, sound absorption and airflow resistance of the pavement surface layers.

Fig. 10 shows comparisons of measured and predicted CPX spectra for different pavements and reference speeds 50 and 80 km/h. Panel (a) shows that the speed effect on a smooth dense surface is well reproduced by the model. The level difference between the two speeds indicates that the speed effect is strongly frequency dependent. This effect is well known for real-world commercial tire fleets as represented in today's road traffic noise emission models by a frequency dependent speed coefficient B_R for rolling noise [14], [15]. In these noise assessment models, the sound power of tire noise clearly increases with speed at all frequency bands ($B_R > 25$ dB). However, it is interesting to note that for the particular CPX case shown in Fig. 10, the speed effect fully vanishes in the 630 Hz 1/3 octave band and even becomes negative at 500 Hz, in both, the measurement and the simulation.

Panel (b) of Fig. 10 shows spectra for two different pavements of the same type. The model accurately reproduces the diverging behavior of the spectra above 630 Hz. The difference between the two pavements at mid and high frequencies is mainly due to the horn effect. Pavement 2 has a lower acoustic impedance than Pavement 1 resulting in a lower horn amplification and in consequence lower CPX levels.

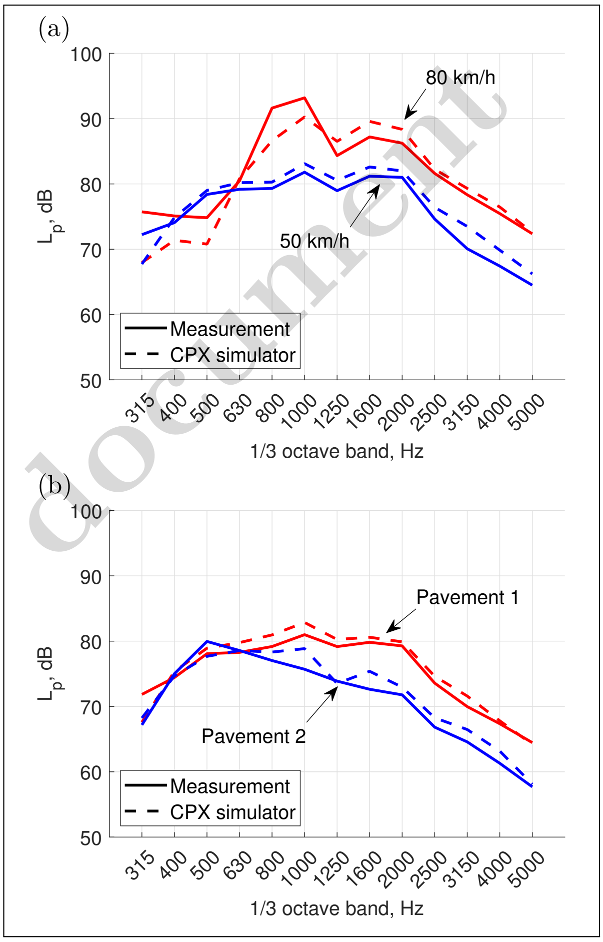

Figure 10: Comparison of simulated and measured CPX spectra with the SRTT on different pavements and reference speeds. (a) Same pavement section (type AC 8) at 50 and 80 km/h. (b) Two different semi-dense asphalt pavements (type SDA 4) at 50 km/h.

5. Conclusions

We presented the concept and first results from the developments of a new hybrid simulation model for the CPX method called CPX simulator. Our work highlights the importance of considering in such a model the influence of the tire tread pattern on sound generation and radiation, the pavement influence on the horn effect, and the influence of the trailer enclosure. First comparisons of calculated and measured CPX spectra for different pavements and speeds show good agreements. The CPX simulator might thus serve as a tool to better understand CPX measurements as well as for the analysis, improvement and design of pavements. Further developments of the model and extending the applications to other pavement types are in progress.

6. Acknowledgments

We thank the Swiss Federal Office for the Environment (FOEN) for the support of this research. The first author also thanks Wolfgang Kropp and Kurt Heutschi for the inspiring discussions.

References

[1] International Organization of Standardization, *ISO 11819-2: Acoustics – Measurement of the influence of road surfaces on traffic noise - Part 2: The close-proximity method*, 2017.

[2] G. Licitra, L. Teti, M. Cerchiai, and F. Bianco, "The influence of tyres on the use of the cpx method for evaluating the effectiveness of a noise mitigation action based on low-noise road surfaces," *Transportation Research Part D: Transport and Environment*, vol. 55, pp. 217–226, 2017, ISSN: 1361-9209.

[3] T. Berge, P. Mioduszewski, M. Hałucha, and J. Bohatkiewicz, "Iso test track influence on the eu tyre label noise value," *Applied Acoustics*, vol. 228, p. 110 315, 2025, ISSN: 0003-682X.

[4] J. H. Kim, K. Kim, O. S. Kwon, W. Y. Cho, and Y. Seo, "Evaluating tire-pavement noise reduction of porous asphalt using close proximity tests: Comparative performance and long-term effectiveness," *Case Studies in Construction Materials*, vol. 23, e05524, 2025, ISSN: 2214-5095.

[5] T. Li, R. Burdisso, and C. Sandu, "Literature review of models on tire-pavement interaction noise," *Journal of Sound and Vibration*, vol. 420, pp. 357–445, 2018.

[6] International Organization of Standardization, *ISO/TS 11819-3: Acoustics – Measurement of the influence of road surfaces on traffic noise - Part 3: Reference tyres*, 2021.

[7] American Society for Testing and Materials, *ASTM F2493-20: Standard Specification for P225/60R16 97S Radial Standard Reference Test Tire*, 2021.

[8] T. Li, "Chapter 2 - tire/road noise separation: Tread pattern noise and road texture noise," in *Automotive Tire Noise and Vibrations*, X. Wang, Ed., Butterworth-Heinemann, 2020, pp. 7–26, ISBN: 978-0-12-818409-7.

[9] Q. Li, F. Ripamonti, R. Corradi, and M. Caccialanza, "Simulation of deterministic tyre noise based on a monopole substitution model," *Applied Acoustics*, vol. 178, p. 108 009, 2021.

[10] W. Kropp, F.-X. Bécot, and S. Barrelet, "On the sound radiation from tyres," *Acta Acustica united with Acustica*, vol. 86, pp. 769–779, 2000.

[11] N.-X. Li, Y.-B. Zhang, C.-X. Bi, and L. Xu, "Experimental study on the horn effect of loaded patterned tires," *Applied Acoustics*, vol. 242, p. 111 053, 2026, ISSN: 0003-682X. DOI: `https://doi.org/10.1016/j.apacoust.2025.111053`

[12] H. Kuttruff, *Room acoustics, 5th edition*. London: Spoon Press, 2009.

[13] International Organization of Standardization, *ISO 10534-2:2023: Acoustics – Determination of acoustic properties in impedance tubes - Part 2: Two-microphone technique for normal sound absorption coefficient and normal surface impedance*, 2023.

[14] "Commission Directive (EU) 2015/996 of 19 May 2015 establishing common noise assessment methods according to Directive 2002/49/EC of the European Parliament and of the Council," European Commission, Brussels, Belgium, Tech. Rep. 2015/996, 2015, Official Journal of the European Union, L 168, 1–823.

[15] K. Heutschi, B. Locher, and M. Gerber, "Sonroad18: Swiss implementation of the cnossos-eu road traffic noise emission model," *Acta Acustica united with Acustica*, vol. 104, pp. 697–706, 2018.